Experimental Investigation of Dissolution Rates of Carbonaceous Materials in Liquid Iron-Carbon Melts

MARCELO B. MOURAO, G.G. KRISHNA MURTHY, and JOHN F. ELLIOTT

Interactions of carbonaceous materials in liquid Fe-C melts have been investigated experimentally by determining the rates of dissolution at temperatures ranging from 1623 to 1935 K. The rates of dissolution of spectroscopic graphite and an industrial coke obeyed the correlation for natural convection under turbulent conditions. The experimental data for the graphite suggested that the rate of dissolution was controlled by mass transfer in liquid boundary layer adjacent to the solid sample. The value of the empirical parameter correlating the dissolution coefficient and the operating variables was found to be 0.19, which was close to that reported in the literature. The comparison of the results obtained for coke and low-volatile coal char samples with those for the graphite revealed that impurities and porosity of the samples can effect the dissolution rates. The values of k_t for coke decreased with increasing the dissolution time. The examination of some of the partially dissolved coke samples by electron microscopy revealed that a thin, viscous ash layer was forming on the sample surface, which must be the main reason for the behavior. The dissolution rates were controlled by both mass transfer and phase boundary reactions when sulfur was present in the bath. The extent of devolatilization and dissolution of coal particles when they were injected into an Fe-C melt depended on the particle size and location.

I. INTRODUCTION

THE injection of carbonaceous materials into liquid iron-carbon alloys has important technological applications, mainly in smelting reduction processes of iron ores and in coal gasification processes in an iron bath. Several smelting reduction processes of iron ores are being developed around the world[1–5] and the most promising one is the in-bath smelting process, where liquid iron-carbon bath is employed to carry out the reduction reactions. The in-bath smelting process is also considered to have many other advantages, such as high productivity, enhanced energy utilization, continuous steelmaking, and easy maneuverable operation. One of the main objectives of such processes is to replace the coke with coals, as the source of carbon, and to avoid the need for an expensive and environmentally troublesome coke-making process.

When coals are added to liquid iron, first they are heated and devolatilized. A gas film will develop around the coal particles during devolatilization, thus avoiding the contact between coal particles and liquid metal.[6] Therefore, the dissolution of carbon into liquid metal from the added carbonaceous particles will take place only after devolatilization. Hence, the interaction of coals with liquid iron-carbon alloys will consist of two processes in series: one being devolatilization and the other being dissolution.

MARCELO B. MOURAO, formerly Visiting Professor, Massachusetts Institute of Technology, is with Polytechnic School, University of Sao Paulo, Sao Paulo, 05508, Brazil. G.G. KRISHNA MURTHY, formerly with the Department of Materials Science and Engineering, Massachusetts Institute of Technology, is with Harvard School of Public Health, Harvard University, Cambridge, MA, 02115. JOHN F. ELLIOT, formerly with the Department of Materials Science and Engineering, Massachusetts Institute of Technology, is deceased.

Manuscript submitted February 10, 1992.

The focus of this investigation has been the interactions of coals with (dissolution of the coal chars in) liquid iron melts. The rate of mass flux, j, of coal char dissolution in the liquid iron-carbon alloy may be defined as

$$j = k_t (C_s - C_b) \quad [1]$$

where C_s and C_b are the carbon concentration at saturation point and of the bulk, respectively. The parameter k_t is the overall dissolution coefficient and is given by

$$\frac{1}{k_t} = \frac{1}{k_m} + \frac{1}{k_b} \quad [2]$$

where k_m is the mass transfer coefficient of carbon in the liquid boundary between solid char and the bulk liquid and k_b is the phase boundary reaction constant.

It is evident from Eq. [2] that the value of k_t depends on the magnitude of the parameters k_b and k_m. If $k_b \gg k_m$, the rate will be controlled by the transport in the liquid boundary layer and vice versa. On the other hand, the rates might be affected by both k_m and k_b if the magnitudes of the two are comparable. The values of k_t have been determined by several investigators by changing the experimental conditions that effect the liquid hydrodynamic conditions around the solid sample (and, in turn, effect k_m). The experimental methods used for the purpose were stationary rods,[7] rotating cylinders,[8–12] revolving discs,[13] and floating carbon particles on the surface of the iron melts.[6,10]

Mass transfer in the boundary layer of the liquid adjacent to the dissolving solid might control the rate of dissolution when Reynold's number is below a certain value,[8–11,13] and the process might be controlled by phase boundary reaction in the higher Reynold's number range.[13] The value of k_b reported in the literature[9,10] was in the range of $5 \times 10^{-3} - 6 \times 10^{-3}$ m/s, and it

was much higher than the values of the overall dissolution coefficients. Several investigators have reported that the impurities (such as sulfur, phosphorus, and oxygen) in the liquid iron-carbon alloy would reduce the dissolution rates.[9,10,11,13] It was, initially, postulated that the diffusion of carbon in the liquid boundary layer adjacent to the solid decreases with increased impurities in the liquid alloy, affecting the dissolution rates of the solid carbon. However, after the comparison of the dissolution rates in impure iron-carbon alloys of pure graphite with those of low-graphitized graphite[9] and of activated carbon,[10] it was evident that the surface of the carbon also effects the rates; the rates decreased further when low-graphitized graphite or activated carbon was used. Therefore, it has been assumed that the impurities in the melt would, perhaps, effect the phase boundary reaction.[9,10,11,13]

Oeters and Orsten[6] and Gudenau *et al.*[12] have investigated the dissolution rates of cokes in the iron-carbon melts, and it has been reported that the dissolution rates of cokes were less than those of pure graphite. It was presumed that the ashes in a coke would reduce the dissolution rates, and that the rates decrease if the melting point of the ashes are higher. A coke with high melting point ash would tend to form a viscous film on the surface, preventing the dissolution.

There have been only a few investigations[6,14] carried out to study the effect of injection parameters on the dissolution rates of carbonaceous materials in iron-carbon alloys. It has been reported[14] that the rates of dissolution of graphite particles were approximately equal to their injection rates until the bath carbon concentration reached 85 pct of the carbon saturation level. The additions of sulfur to the melt decreased the dissolution rate.[14] Oeters and Orsten[6] showed that the dissolution rate depended strongly on the particle size and carbon content of the melt.

The authors of this article, therefore, have carried out a set of experiments to study the rates of dissolution of different types of carbonaceous materials in the liquid iron-carbon alloys. The method of the experiments is presented in Section II followed by results and discussions in Section III. Several experiments were also conducted to study the extent of devolatilization and dissolution of different types of coal particles when they were injected into liquid iron-carbon alloys, and the results of those experiments are discussed in Section IV.

II. EXPERIMENTAL

Experiments to study the dissolution rates of carbonaceous materials in 300 g of iron-carbon alloys, contained in a pure (99.8 pct) alumina crucible of 35 mm inner diameter and 120-mm-long, were carried out at temperatures ranging from 1623 to 1935 K. The iron-carbon melts were prepared, in an induction furnace, by melting a mixture of pure electrolytic iron and graphite powder. The furnace was heated using a pure graphite susceptor in which the alumina crucible was placed. The experimental setup employed in the present investigations is shown in Figure 1. The furnace temperatures were monitored using a type-B thermocouple which was placed between the graphite susceptor and the alumina crucible. The initial carbon concentration of the iron-carbon baths ranged between 0.5 and 3.5 wt pct C. The furnace was continuously purged with argon gas during the experiments at a flow rate of 7.17×10^{-6} m^3/s.

The behavior of carbonaceous materials in iron-carbon melts was examined by conducting several experiments using samples of pure spectroscopic graphite, industrial coke, and coal chars (obtained from anthracite and low volatile bituminous coals whose proximate analysis is given in Table I). The spectroscopic graphite samples were cylindrical in shape (4.53 mm in diameter and 1873 kg/m^3 of density) and contained less than 1 parts per million (ppm) ash and less than 6 ppm impurities with maximum 2 ppm per element. The cylindrical industrial coke and coal char samples (10–20 mm in diameter and 20–30 mm in length) were obtained by grinding large pieces of coke and coal char. The coke samples were devolatilized at 1723 K before they were used for the dissolution studies. The anthracite coal char samples were acquired after devolatilizing the coal samples under argon atmosphere by heating slowly to 1723 K. Similarly, low volatile bituminous coal char samples were prepared by slowly heating the coal samples to 1723 K under argon atmosphere, initially at a rate of 100 K/h until the sample reached 873 K and then at a rate of 300 K/h.

The carbon samples were preheated for about 120 s before they were immersed into the melt by holding with an alumina rod. The samples were immersed in the iron-carbon melt for a known amount of time (10 to 150 s) and were withdrawn from the melt. The partially dissolved samples were furnace-cooled by holding them in the low-temperature zone. The amount of carbon dissolved in the melt was determined from the weight-loss measurements of the samples. Several dissolution experiments were carried out employing the same iron-carbon melt, and the carbon content of the melt was determined for each dissolution experiment by analyzing samples of the melt for carbon after each dissolution experiment.

The interaction of different types of coals with iron-carbon melts was studied using different size coal powders, which were dropped onto the melt surface (powders were freely floating on the surface of the melt) or injected into a bath. The experiments were carried out by measuring the flow rate of devolatilized gases and by determining the bath carbon composition. The results of the experiments are presented and discussed below.

III. RESULTS AND DISCUSSIONS

The rates of dissolution of various carbonaceous materials (spectroscopic graphite, industrial coke, and coal chars) were determined using the weight-loss measurements of the dissolved samples. The total weight of the carbon dissolved, W_{cd}, in the melt was determined by multiplying the measured weight loss of the sample with the fixed carbon of the material at the experimental temperature. Equation [1] was rewritten to calculate the rate constant for dissolution, k_t,

$$k_t = \frac{W_{cd}}{t\, A_s\, (C_s - C_b)} \qquad [3]$$

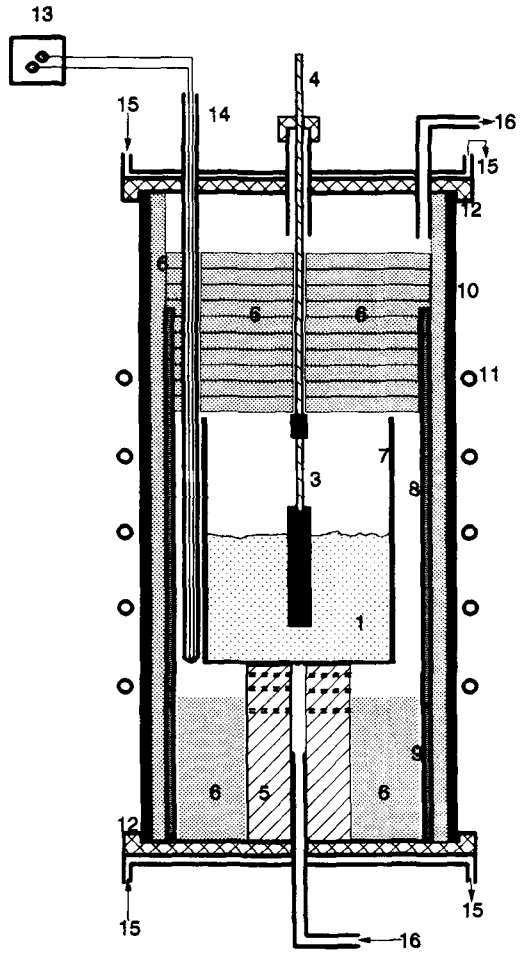

1 Iron-Carbon Melt
2 Carbonaceous Sample
3 Alumina Rod
4 Graphite Tube
5 Crucible Stand (Graphite)
6 Graphite Felt for Insulation
7 Alumina Crucible
8 Graphite Suceptor
9 Suceptor Stand (Graphite)
10 Silica Furnace Tube
11 Induction Coil
12 Brass Furnace Lid
13 Thermocouple
14 Thermocouple Protection Tube
15 Cooling Water
16 Argon

Fig. 1—Schematic diagram of the experimental setup used in the dissolution experiments.

where t is the total immersion time of the sample and A_s is the apparent surface area of the immersed part of the sample, which was estimated using the average diameter calculated based on initial and final diameters of the sample. The final diameter, d_f, of the immersed part of the sample was calculated using the following equation:

$$d_f = \sqrt{d_i^2 - \frac{4W_{cd}}{\pi L \rho_c}} \qquad [4]$$

where d_i is the initial diameter of the sample, L is the immersed length of the sample, and ρ_c is the density of the sample.

Some typical values of the experimentally determined coefficients of rate of dissolution, k_t, are presented in Tables II and III. The results in Table II are for graphite and those in Table III are for an industrial coke whose proximate analysis is given in Table I. The values of k_t determined in the present investigation have varied between 8.3×10^{-5} and 20.6×10^{-5} m/s for spectroscopic graphite; between 1.8×10^{-5} and 28.1×10^{-5} m/s for coke; 5×10^{-5} and 35×10^{-5} m/s for anthracite coal char; and 4×10^{-5} and 14×10^{-5} m/s for low volatile bituminous coal char. The values were functions of bath temperature, carbon content, and sample immersion time, t_I.

An attempt was made to compare the experimentally determined values of k_t obtained using spectroscopic graphite with those derived using industrial coke or coal char samples at different operating variables. The operating variables that were investigated in the present study have been the bath carbon concentration, temperature, and agitating rates. It is well known that the bath density, which influences the hydrodynamic conditions, depends on both carbon concentration and temperature. The values of k_t will also be affected by chemical activity in the bath. The parameters k_m and k_b (given in Eq. [2]) represent the contribution of physical conditions and chemical activities in the bath, respectively, to the overall dissolution process. Thus, the values of parameters k_m and k_b as functions of operating parameters need to be determined before any comparisons can be made.

The relationship between the value k_m and hydrodynamic conditions of the bath was deduced from the available dimensionless correlations.[7] Under the present experimental conditions, the hydrodynamic conditions near the sample might be governed by natural convection. For a cylindrical sample in its vertical position, the dimensionless correlation under natural convection may be written[7] as

$$\mathrm{Sh} = 0.555\,(\mathrm{Gr}_m\mathrm{Sc})^{1/4} \text{ for } 10^4 < \mathrm{Gr}_m\mathrm{Sc} < 10^8 \qquad [5]$$

and

$$\mathrm{Sh} = 0.129\,(\mathrm{Gr}_m\mathrm{Sc})^{1/3} \text{ for } 10^8 < \mathrm{Gr}_m\mathrm{Sc} < 10^{12} \qquad [6]$$

Table I. Proximate Analysis of the Carbonaceous Materials Used in the Present Investigation

Material Type	As-Received				Dry, Ash-Free	
	Moisture	Ash	Volatile Matter	Fixed Carbon	Volatile Matter	Fixed Carbon
Coke	1.3	8.3	4.3	86.1	4.7	95.3
Anthracite	0.3	2.9	3.9	92.9	4.0	96.0
Low volatile	1.5	6.4	13.8	78.3	15.0	85.0
Medium volatile	1.8	3.2	19.8	75.1	20.8	79.2
High volatile	2.2	4.2	33.9	59.6	36.3	63.7

Table II. A range of Operating Conditions and Some Typical Experimentally Determined Values of Dissolution Coefficients for Graphite

T (K)	Wt Pct C	L (mm)	d_i (mm)	t (s)	W_{cd} (g)	k_t, × 10^4 (m/s)
1770	2.3	34.4	4.53	25	0.189	0.90
1796	0.8	27.4	4.53	20	0.222	1.07
1807	0.8	13.5	4.53	20	0.135	1.33
1853	0.9	9.1	4.53	30	0.162	1.82
1875	1.5	10.6	4.53	25	0.152	1.96

Table III. A Range of Operating Conditions and Some Typical Experimentally Determined Values of Dissolution Coefficients for Coke

T (K)	Wt Pct C	L (mm)	d_i (mm)	t (s)	W_{cd} (g)	k_t, × 10^4 (m/s)
1747	1.5	29.68	12.09	25	0.530	0.85
1777	1.0	22.32	11.14	20	0.661	1.76
1797	1.6	18.45	11.52	30	0.475	1.14
1818	0.5	25.26	10.61	30	0.665	0.96
1845	2.0	23.19	11.40	20	0.721	2.31

where Sh (Sherwood number), Gr_m (Grashof number), and Sc (Schmidt number) are defined, respectively, as

$$Sh = \frac{k_m L}{D_c} \quad [7]$$

$$Gr_m = \frac{g\Delta\rho\rho_s^2 L^3}{\mu^2} \quad [8]$$

and

$$Sc = \frac{\mu}{\rho_s D_c} \quad [9]$$

Where L is the immersed length of the sample, D_c is the diffusion coefficient of the carbon in the liquid iron-carbon alloys, g is the acceleration due to gravity, ρ_s is the density of the carbon-saturated iron melt, μ is the melt viscosity, and $\Delta\rho$, buoyancy factor, is given by

$$\Delta\rho = \frac{\rho - \rho_s}{\rho} \quad [10]$$

where ρ is the melt bulk density.

The value of $Gr_m Sc$ for a carbon sample 15-mm-long, immersed in a bath having 1 pct carbon at 1823 K, was 2×10^8 (the values of ρ, μ, and D_c used in the calculations were estimated employing the correlations given in the Appendix). Therefore, the correlation given by Eq. [6] will be applicable for the set of operating conditions employed in the present investigation. Hence, the parameter k_m can be expressed in terms of several variables as follows:

$$k_m = a\left(\frac{g\Delta\rho\rho_s}{\mu}\right)^{1/3} D_c^{2/3} \quad [11]$$

where a is an empirical coefficient. The important feature of the equation is that the values of parameter k_m do not depend on the characteristic length, L.

With the substitution of Eq. [11] in Eq. [2], assuming that the parameter k_b is a constant for a given set of experimental conditions, one would obtain a linear relationship between the dissolution coefficient, k_t, and the operating variables. Therefore, a plot of $1/k_t$ *vs* $[g\ \Delta\rho/\rho_s\mu]^{-1/3}\ D_c^{-2/3}$ would give a straight line with a slope of $1/a$ and a constant (Y-intercept) which will be equal to $1/k_b$. If the process is controlled only by mass transfer, as was reported by several investigators,[7–12] the value of $1/k_b$ should be negligible when compared to that of $1/k_m$. Therefore, the intercept would be negligible or close to zero, and the plot of k_t *vs* $[g\ \Delta\rho\ \rho_s/\mu]^{1/3}\ D_c^{2/3}$ with zero intercept would be a straight line whose slope would be equal to the value of the parameter a. Figure 2, obtained for pure spectroscopic graphite, indeed depicts the argument. The obtained value of the parameter a was

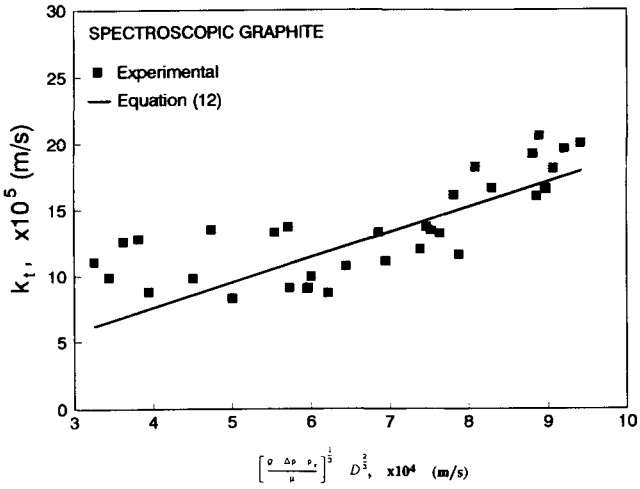

Fig. 2—A plot of experimentally determined dissolution coefficient, k_t, *vs* $[g\Delta\rho\rho_s/\mu]^{1/3}\ D^{2/3}$ for spectroscopic graphite.

0.19, which was close to the values reported in the literature[7] (0.129 and 0.11). Thus, the following correlation can be taken as the basis for the comparison of the data obtained for industrial cokes and coal chars with those obtained using spectroscopic graphite:

$$k_t = 0.19\left(\frac{g\Delta\rho\rho_s}{\mu}\right)^{1/3} D_c^{2/3} \qquad [12]$$

Figure 3 shows a plot of k_t *vs* $[g\ \Delta\rho\ \rho_s/\mu]^{1/3}\ D_c^{2/3}$ for industrial coke, anthracite coal char, and low volatile bituminous coal char. It was evident from the plot that the data for coke and coal char samples were scattered around the line given by Eq. [12]. The data obtained using coke samples (Figure 6) for immersion times (t_I) less than 30 s were higher and those for t_I more than 30 s were lower than the values calculated employing Eq. [12]. Oeters and Orsten[10] and Gudenau *et al.*[12] have also observed that the dissolution rates for coke decreased with increasing immersion time. The initial high dissolution rate for the coke samples employed in the present study probably was due to the higher effective surface area available for dissolution because of the porous structure of the coke. The data points for anthracite and low volatile coal chars were obtained for the immersion times less than or equal to 30 s. The data for anthracite coal char were scattered around the line given by Eq. [12]; therefore, it may be assumed that the dissolution coefficient for anthracite coal char was similar to that of coke samples. On the other hand, the values of dissolution coefficients for low volatile bituminous coal char samples were less than those determined by Eq. [12].

The scatter in the data points for coke and coal char samples must have been due to the fact that the ash content and porous structure of the samples play a role in the dissolution process. Several partially dissolved coke samples were examined by electron microscopy, and the slag-like surface was analyzed for its chemical composition. A few typical micrographs are presented in Figure 4. The structure of the unreacted coke sample surface was comparatively smoother (micrograph I) and that of the partially reacted sample surface was porous and covered with molten slag phase (micrographs II and III). Gudenau *et al.*[12] as well as Oeters and Orsten[6] have made similar observations.

The chemical analysis of the slag-like layer on the partially reacted two coke samples is given in Table IV. It

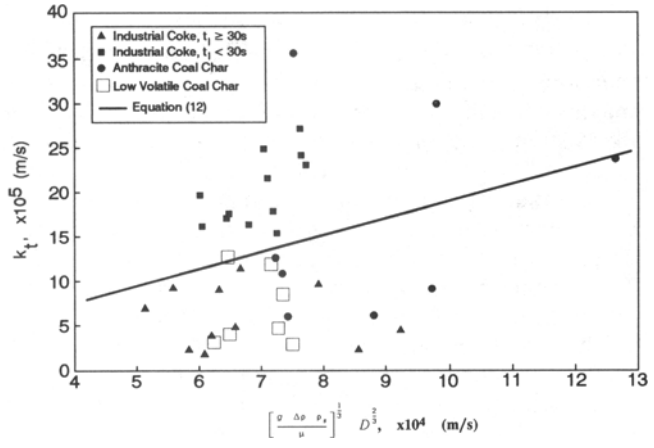

Fig. 3—Comparison of values of dissolution coefficient, k_t, determined experimentally for coke, anthracite coal char, and low volatile coal char with those estimated using Eq. [12].

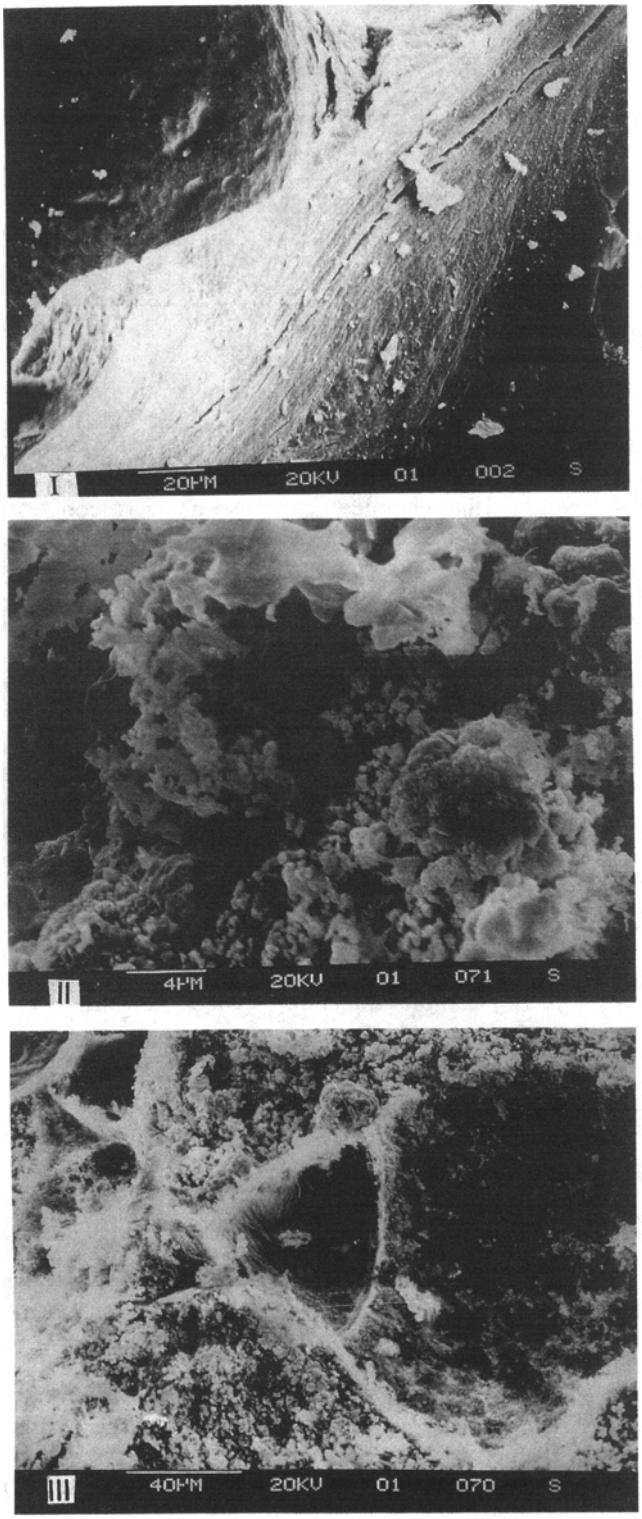

Fig. 4—Micrographs of surface of some partially dissolved coke samples: (I) before dissolution; (II) after 25 s; and (III) after 210 s.

Table IV. Chemical Composition of Slag-like Layer Found on Partially Dissolved Coke Samples Obtained from Microanalysis

	Elemental Analysis (Wt Pct)							
	Fe	Al	Ca	Si	K	Na	Ti	P
Sample 1								
At a point	68.4	22.1	1.6	4.7	0.6	2.6	—	—
Average	54.9	29.8	1.8	5.9	1.8	5.0	0.8	—
Sample 2								
At a point	36.9	26.1	1.5	4.2	0.5	—	1.1	0.6
Average	31.5	38.1	0.2	2.1	0.3	0.8	0.8	—
	Oxides, Estimated Using Elemental Analysis (Wt Pct)							
	Al_2O_3	CaO	SiO_2	K_2O	Na_2O	TiO_2	P_2O_5	
Sample 1								
At a point	71.8	3.9	17.0	1.1	6.0	—	—	
Average	69.0	3.1	15.4	2.7	8.3	1.6	—	
Sample 2								
At a point	76.7	3.2	14.1	0.9	—	3.0	2.0	
Average	91.1	0.3	5.6	0.5	0.6	1.9	—	

can be seen in the table that the slag layer on the partially reacted coke samples primarily contained metallic iron and aluminum. It was assumed that all of the elements other than iron were present in the form of slag, and accordingly the chemical composition was converted into oxides. The slag layer contained about 70 to 90 wt pct Al_2O_3; about 6 to 17 wt pct SiO_2; approximately 0.3 to 4 wt pct CaO; and traces of TiO_2, Na_2O, K_2O, and P_2O_5. Therefore, it can be concluded that the slag-like viscous layer was slowing down the dissolution process. As the dissolution proceeds, the ash content on the surface of the sample increases, leading to the formation of a thick viscous layer which will reduce the surface area available for dissolution. In addition, the liquid metal that penetrated into the pores of the sample in the beginning of the process might be trapped inside the pores. If so, the pores may become saturated with carbon, limiting the dissolution of carbon in the coke into the liquid alloy.

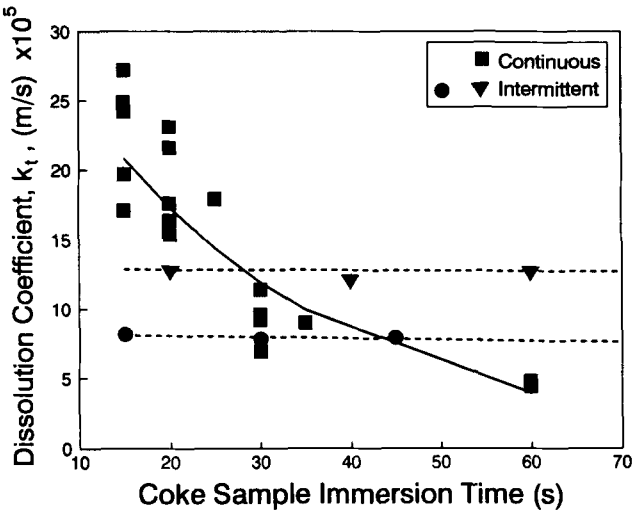

Fig. 5—Variation of dissolution coefficient, k_t, as a function of dissolution time (for less than 60 s) for coke samples immersed continuously or intermittently.

A. *Effect of Sample Immersion Time, t_I, on the Dissolution Rates*

The effects of the formation of a viscous layer and the penetration of molten iron into the sample pores on the dissolution rates were investigated by conducting experiments with a coke sample which was immersed intermittently several times. The partially reacted sample was withdrawn after several seconds, cooled to room temperature, and weight lost due to dissolution was determined to estimate the dissolution coefficient, k_t. The sample was reimmersed into the bath for a known period, and the process was repeated several times. The values of k_t were determined after each immersion based on the weight lost during the total time period (cumulative weight loss).

The values of k_t determined in these experiments for three different coke samples are compared with those obtained employing the data from the continuous immersion experiments in Figures 5 and 6. The data in Figure 5 were obtained for the immersion times less than 60 s and those in Figure 6 were for the immersion times more than 30 s. The total length of immersion did not effect the determined values of k_t in the intermittent immersion experiments; the values of k_t were approximately constant with the time of immersion. Thus, the dissolution process continued at a constant rate after each cycle. However, the values of k_t determined from the continuous immersion experiments were monotonically decreased with increased immersion time, t_I. It was presumed that the viscous slag layer formed during the dissolution process was changing its morphology while cooling, leading to renewed active surface.

The calculated amounts of carbon dissolved into Fe-C melts employing W_{cd} were verified with measurements of the actual carbon content of the bath. The bath carbon content was determined from the chemical analysis of the melt samples obtained after each dissolution experiment. Figure 7 shows the comparison of the bath carbon composition determined employing chemical analysis of

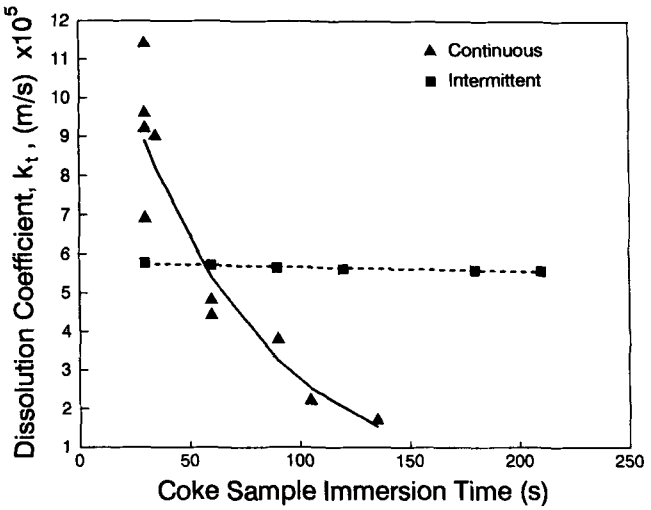

Fig. 6—A plot of dissolution coefficient, k_t, *vs* dissolution time (for more than 30 s) for coke samples immersed continuously or intermittently.

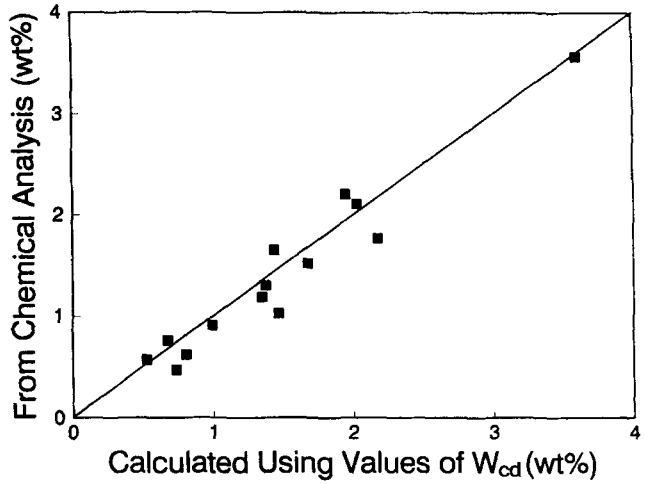

Fig. 7—Comparison of bath carbon composition determined through chemical analysis with that calculated using the values of W_{cd}.

the melt samples with that calculated using the value of W_{cd}. The agreement between the values of the bath carbon content obtained using the two methods was excellent.

B. *Effect of Sulfur on the Dissolution Rates*

Although it was mentioned earlier that the phase boundary reactions were not rate-limiting, the presence of surface-active elements, such as sulfur, may retard phase-boundary reaction rates. Therefore, the value of k_b in the presence of surface-active elements will be less than that without sulfur, and hence the contribution of k_b in the presence of surface active elements to the overall dissolution coefficient, k_t, will be considerable. This was examined by determining the values of k_t for spectroscopic graphite and industrial coke samples dissolving in sulfur containing Fe-C bath. Figure 8 shows the effect of sulfur on the values of k_t obtained by conducting experiments with 0.28 and 0.93 wt pct S melts using spectroscopic graphite and coke samples. The values of k_t

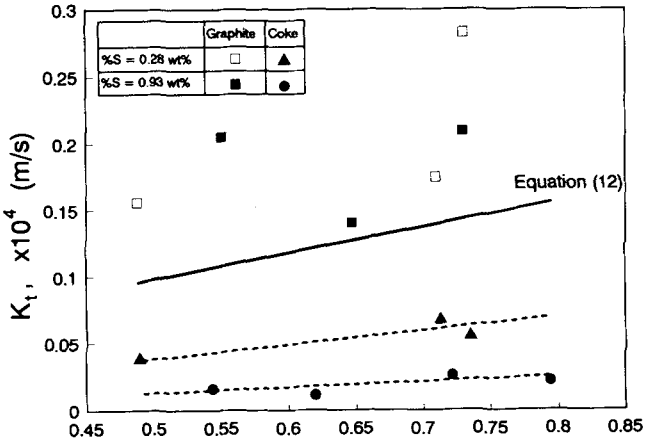

Fig. 8—Effect of bath sulphur content on the dissolution coefficient, k_t, for spectroscopic graphite and coke samples.

for graphite were larger than those expected for sulfur-free melts. However, the data points obtained for 0.93 pct S were no different from those for 0.28 pct S. Kalvelage *et al.*[15] have reported similar observations. It was believed that the wettability of graphite by Fe-C melts increases with increasing sulfur in the bath, which might lead to increased rates of dissolution. On the other hand, the values of k_t determined from the experiments using coke samples in sulfur containing melts were less than those obtained with sulfur-free melts, and the values of k_t decreased further with an increased amount of sulfur in the bath. Similar conclusions can be drawn after comparison of the data reported for graphite[9] with those for coke.[10] If the hydrodynamic conditions were controlling the dissolution rates, the effect of sulfur on the dissolution of graphite and coke would have been the same because of the fact that the change in the melt physical properties (density and viscosity) of the melt having a known amount of sulfur will be constant. Therefore, it may be concluded that the phase boundary reactions were playing a role when sulfur was added to the bath.

The retarding effect of sulfur was more pronounced in coke than it was in graphite because of the differences in the surface structure. The high degree of graphitization of pure graphite offers less active sites, which lowers sulfur adsorption kinetics. Several experiments were performed to investigate the effect of bath agitating rates on the graphite surface reactions, both in the sulfur-free and sulfur-containing melts. The bath was agitated by injecting argon gas in the range of 0 to 13.33 $\times$ 10^{-5} Nm^3/s. The results of the experiments conducted using sulfur-free and 0.84 pct S sulfur-containing melts are shown in Figure 9. As shown, the values of k_t increased with increasing bath agitation rates. However, the values of k_t obtained using sulfur-containing melts did not increase at the same rate as those employing sulfur-free melts in the range of gas-flow rates employed in the present study. This might be possible only if the sulfur adsorption rate on the graphite surface increased with increasing turbulent intensity of the bath.

C. *Interaction of Coal Particles with Fe-C Melts*

Behavior of various types of coal particles in liquid iron-carbon alloys was examined by conducting two

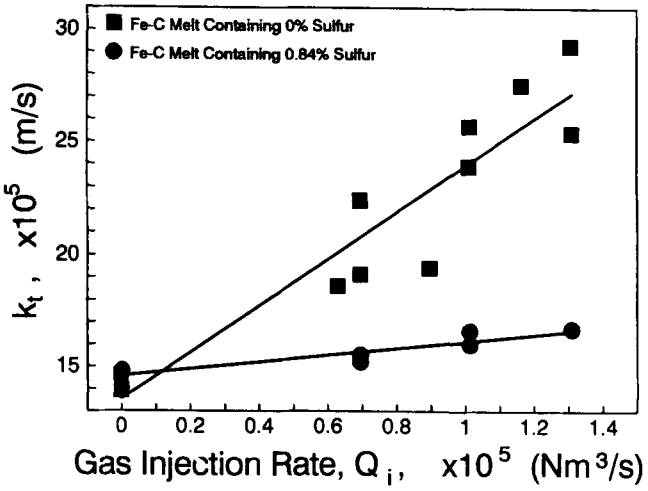

Fig. 9—A plot showing the effect of sulfur in the bath on the experimentally determined values of dissolution coefficient, k_t, for spectroscopic graphite *vs* gas flow rate, Q_i.

types of experiments with particulate coal additions to a liquid bath of 1.5 kg contained in a pure alumina crucible of 78.8 mm in diameter and 165-mm-long. The experiments were carried out at 1823 K. In the first set of experiments, the coal particles ranging from 2 to 5.6 mm in size were dropped onto the melt surface, whereas those in the second set, the coal particles from 0.6 to 1.2 mm in size, were injected into the bath. The coal particles were injected through an alumina tube 5 mm in diameter, and argon was used as carrier gas at a flow rate of 10.2×10^{-6} Nm^3/s. The extent of devolatilization was determined by measuring the gas-flow rates. Some typical values of volume of gas evolved are presented in Table V. The amount of gas volumes measured in these experiments was much less than that determined in the devolatilization experiments[16] (they were about 30 to 59 pct of gas volumes obtained in devolatilization experiments), which might be partly due to measurement errors and because a lot of unreacted particles were carried away from the reactor by the carrier gas. The carbon recovery was determined using the melt carbon composition which was obtained from the chemical analysis of the melt samples taken before and after each experiment. The carbon recovery was only about 77 and 59 pct in the surface addition and injection experiments, respectively.

IV. CONCLUSIONS

Rates of dissolution of spectroscopic graphite, industrial coke, and coal (anthracite and low-volatile bituminous coal) chars were determined under natural and forced convections by determining weight loss of the samples. The values of dissolution coefficient, k_t, determined under natural convection were controlled only by mass transport, and the contribution of phase boundary reactions was negligible. The values of k_t for coke decreased with increasing dissolution time. The examination of some of the partially dissolved coke samples under an electron microscope revealed that a thin (viscous) ash layer was forming on the sample surface, which must be the main reason for the behavior.

The values of k_t were affected by both sulfur in Fe-C melt and turbulent intensity of the bath (the rates decreased with increasing sulfur in the bath or by decreasing the turbulent intensity of the bath). Therefore, it was concluded that the dissolution rates were controlled by both mass transfer and phase boundary reactions when surface active elements, such as sulfur, were present in the bath or when the bath was stirred. The effect of phase boundary reactions on the dissolution of coke and coal chars in sulfur-containing melts was more than that on the dissolution of spectroscopic graphite in the same melts.

The extent of devolatilization and dissolution of different types of coal particles, either dropped onto the bath surface (freely floating on the surface) or injected into the bath, was determined at 1823 K. The measured volumes of volatilization gases were about 30 to 59 pct of those determined in the high-temperature devolatilization experiments. The carbon recovery in these experiments was about 77 pct when the particles were dropped onto the bath surface and about 59 pct when the particles were injected into the bath.

APPENDIX

PROPERTIES EVALUATION

The carbon concentration, C_s, and density, ρ_s, of the melt at carbon saturation were evaluated using the following expressions available in the literature,[10]

Table V. Extent of Devolatilization of Medium Volatile Coal Particles, Either Dropped onto the Melt Surface ($Q_1 = 0$) or Injected ($Q_1 > 0$), when They were Interacting with Fe-C Melts at 1823 K

Gas Injection Rate $Q_1 \times 10^5$ (Nm^3/s)	Sample Weight (g)	Particle Size (mm)	Estimated Volatile Gases $\times 10^3$ (m^3)	Experimental Volatile Gases $\times 10^3$ (m^3)
0.0	1.00	2–2.36	0.87	0.26
0.0	1.00	3.2–5.6	0.87	0.44
0.0	2.01	3.2–5.6	1.75	0.73
1.02	1.70	0.59–0.707	1.48	0.65
1.02	2.06	0.707–1	1.79	1.05
1.02	2.39	1–1.19	2.08	0.94

$$C_s = 1.34\,2.54 \times 10^{-4}(T - 273) - 0.4(\text{wt pct S}) \quad [AI.1]$$

and

$$\rho_s = 8750 - 69.6(\text{wt pct C}) - 1.15(T - 273) \quad [AI.2]$$

where wt pct C and wt pct S are the weight percentages of carbon and sulfur of the melt. The viscosity, μ, of liquid iron-carbon alloys depends both on temperature and melt carbon concentration. The values of viscosity corresponding to the liquid in the boundary layer adjacent to the carbon surface, where it will be carbon-saturated, were of significance to the present investigations and were obtained[7] by extrapolating the data available for low-carbon melts to the level of carbon saturation, which is given by

$$\mu = 10^{-5.31+4874/T} \quad [AI.3]$$

The value of the carbon diffusion coefficient, D_c, in liquid carbon-saturated iron alloys was not available; several correlations have been proposed to estimate the same.[17] The general format of these correlation was given by

$$D_c = \alpha \frac{T}{\mu} \quad [AI.4]$$

where the parameter α is a constant. The value of α was determined after employing the reported[7] values of D_c and the values of μ, given by Eq. [AI.3], and it was found to be 2.5×10^{-14}.

LIST OF SYMBOLS

A_s	surface area of the dissolving sample (m^2)
a	empirical coefficient defined by Eq. [11] (dimensionless)
C_b	carbon concentration of the bath (kg/m^3)
C_s	carbon concentration of carbon-saturated bath (kg/m^3)
D_c	carbon diffusion coefficient in Fe-C melts (m^2/s)
d_f	sample final diameter (m)
d_i	sample initial diameter (m)
Gr_m	Grashof number for mass transport (dimensionless)
g	acceleration due to gravity (m/s^2)
j	mass flux per unit surface area of the sample (kg/m^2s)
k_b	phase-boundary reaction constant in Fe-C melts (m/s)
k_m	mass transfer coefficient (m/s)
k_t	overall dissolution coefficient (m/s)
L	sample length (m)
n	empirical constant in Eq. [1] (dimensionless)
Sc	Schmidt number (dimensionless)
Sh	Sherwood number (dimensionless)
T	temperature (K)
t	time (s)
t_I	sample immersion time (s)
W_{cd}	weight of carbon dissolved (kg)
α	empirical constant in Eq. [AI.4] ($m \cdot kg/K \cdot s^2$)
$\Delta\rho$	buoyancy factor defined by Eq. [10] (dimensionless)
μ	melt viscosity (kg/ms)
ρ	melt bulk density (kg/m^3)
ρ_c	sample density (kg/m^3)
ρ_s	carbon-saturated melt density (kg/m^3)

ACKNOWLEDGMENTS

The authors express their appreciation to the Brazilian Research Council (CNPq), to the American Iron and Steel Institute, and to the Department of Energy (DOE Cooperative Agreement No. DE-FC07-89ID12847) for financial support of this work.

REFERENCES

1. Y. Hayashi, M. Nakamura, and N. Tokumitsu: *Process Technology Conference Proceedings*, Iron and Steel Society, Inc., Warrendale, PA, 1986, vol. 6, Book 3, pp. 1057-64.
2. G.J.W. Kor: *Steel Res.*, 1989, vol. 60, pp. 122-24.
3. H.A. Fine, R.J. Fruehan, Dieter Janke, and Rolf Steffen: *Steel Res.*, 1989, vol. 60, pp. 188-90.
4. J.O. Edstrom, J. Ma, and J. Von Scheele: *Nordic Steel Min. Rev.*, 1990, pp. 24-34.
5. F. Oeters and E. Gorl: *Steel Res.*, 1990, vol. 61, pp. 385-400.
6. S. Orsten and F. Oeters: *Process Technology Conference Proceedings*, Iron and Steel Society, Inc., Warrendale, PA, 1988, vol. 8, pp. 31-42.
7. M. Kosaka and S. Minowa: *Trans. Iron Steel Inst. Jpn.*, 1968, vol. 8, pp. 392-400.
8. R.G. Olsson, V. Koump, and T.F. Perzak: *Trans. Met. Soc. AIME*, 1966, vol. 236, pp. 426-29.
9. Y. Shigeno, M. Tokuda, and M. Ohtani: *Trans. Jpn. Inst. Met.*, 1985, vol. 26, pp. 33-43.
10. S. Orsten and F. Oeters: *Process Technology Conference Proceedings*, Institute for Scientific Information, Philadelphia, PA, 1986, vol. 6, Book 3, pp. 143-55.
11. S.-O. Ericsson and P.-O. Mellberg: *Scand. J. Metall.*, 1972, vol. 1, pp. 57-61.
12. H.G. Gudenau, J.P. Mulanza, and D.G.R. Sharma: *Steel Res.*, 1990, vol. 61, pp. 97-104.
13. V.A. Grigoryan and V.P. Karshin: *Russ. Metall.*, 1972, vol. 1, pp. 57-59.
14. J.K. Wright and B.R. Baldock: *Metall. Trans. B*, 1988, vol. 19B, pp. 375-82.
15. L. Kalvelage, J. Markert, and J. Poetschke: *Arch. Eisenhüttenwes.*, 1979, vol. 50, pp. 107-10.
16. Marcelo B. Mourao, G.G. Krishna Murthy, and John F. Elliott: "Interaction of Carbonaceous Materials with Liquid Iron-Carbon Alloys," *EPD-Congress*, TMS-AIME, Warrendale PA, March 1992, pp. 807-20.
17. T. Iida and R.I.L. Guthrie: *The Physical Properties of Liquid Metals*, Oxford University Press, Oxford, 1988, pp. 216-25.